MINERvA's Medium Energy Physics Program

MINERvA collaboration

December 22, 2014

Abstract

This document outlines the physics program that MINERvA will pursue by taking data in the Medium Energy beam. It describes the measurement capabilities of the experiment assuming an exposure of 10×10^{20} protons on target in neutrino running and 12×10^{20} protons on target in antineutrino running.

1 Executive Summary

The goal of the MINERνA physics program is to measure the effects of the nucleus on a wide range of neutrino interactions, for a wide range of nuclei. By making measurements on nuclei both lighter and heavier than those used to oscillation experiments, MINERνA can test the models of nuclear effects that are crucial for precision oscillation measurements. Since nuclear effects may be different between neutrinos and antineutrinos, and because oscillation experiments ultimately will measure both probabilities to study CP violation and neutrino mass hierarchy, MINERνA needs a substantial antineutrino exposure. A Medium Energy exposure of 10×10^{20} (12×10^{20}) in neutrino (antineutrino) mode will provide a factor of 10 (25) increase in event statistics above the Low Energy neutrino (antineutrino) exposures collected, thereby enabling MINERνA to make measurements of a wide range of interaction channels on a wide range of nuclei, from carbon to lead.

The fine granularity of the MINERvA detector[1] and the high intensity of the NuMI beam represent an excellent opportunity to make measurements of neutrino interactions in the 2-8 GeV range. This is an important energy range because it includes the the signal region for the NOvA and LBNF neutrino oscillation experiments. It is also the neutrino energy range that gives

rise to feed-down of background processes for the oscillation experiments T2K and NOvA. This energy range is also interesting from the perspective of neutrino-nucleus scattering as a probe of nuclear physics. The different channels available in neutrino scattering, from quasielastic to resonance production to deeply inelastic, are all produced at significant rates.

MINERvA has an ongoing physics program to analyze and publish results from the Low Energy data, whose energy peaks at about 3 GeV and which includes approximately 3×10^{20} protons on target (POT) in neutrino mode and 1.5×10^{20} POT in antineutrino mode. Because of the relatively low statistics in that exposure, MINERνA has so far only made inclusive measurements of nuclear effects in neutrino mode. MINERvA's program also includes collecting Medium Energy neutrino data, with peak neutrino energy of 7 GeV, and demonstrating that the detector has the same high reconstruction capability as was seen in the Low Energy data in spite of the much increased instantaneous event rates.

This document reviews the physics justification for precision neutrino interaction measurements and then summarizes the Low Energy physics milestones that MINERνA has achieved. The next section describes a few studies done recently that assess and confirm the Medium Energy data that MINERνA is currently collecting is of high quality. This secion provides projections for the capabilities of the expected Medium Energy data for speciic channels, using our hit-level simulation which has been benchmarked with the Low Energy data. Given the importance of this physics, the current and projected performance of the MINERνA detector, and the investment in the detector and collaboration to date, the case to continue MINERνA operations to allow for the collection of the full, expected Medium Energy data is straightforward and compelling.

2 The Physics Potential of Medium-Energy ν and $\bar{\nu}$ Exposures using MINERνA

The Medium Energy beam offers a unique opportunity to do high statistics measurements in a range of neutrino energies, considerably beyond that is accessible through the Low Energy data. Figure 1 shows the neutrino and antineutrino fluxes for the Low and Medium Energy beam tunes in units of neutrinos per POT. While there is some overlap between the energy ranges

accessible, the integrated neutrino flux per proton on target is a factor of 2.3 (2.1) larger in Medium Energy beam than in the Low Energy beam in neutrino (antineutrino) mode. For processes whose cross section scales linearly with neutrino energy, the expected event rate is closer to a factor of 3.4 (3.3) greater in the Medium Energy beam.

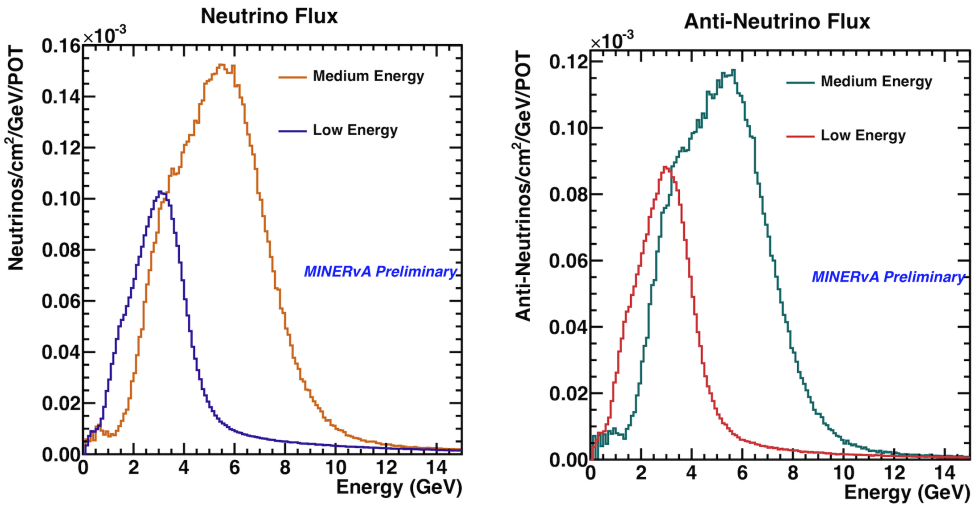

Figure 1: Neutrino (antineutrino) fluxes per proton on target as a function of Energy, for both the Low Energy and Medium Energy tunes of the NuMI beamline, as predicted by a GEANT4 simulation reweighted using results from the NA49 hadron production experiment.

2.1 Exclusive Measurements

New physics searches with neutrinos are highly sensitive to the accuracy of neutrino energy reconstruction. CP-violation and sterile neutrinos will manifest as distortions in the measured energy spectrum. It is important to understand the overall level of the interaction probability as well as the fine kinematics of the event because the shape of the energy distribution is influenced by the event reconstruction strategy.

Neutrino experiments are in the difficult position of lacking event-by-event knowledge of the incoming neutrino energy. This puts heavy reliance on the physics models in the event generator to produce an appropriate energy

estimator and to predict background levels. It is possible to apply some constraints from electron scattering experiments. But the fact that charged-lepton scattering experiments are only capable of describing the vector part of the interaction limits their relevance to exclusive channels in neutrino scattering, which are also sensitive to the axial-vector part.

For the purposes of building models capable of providing precision energy estimators, very careful exclusive-state measurements are invaluable. Inclusive measurements alone are not sufficient to build a full interaction model because exclusive channels offer unique handles for disentangling competing nuclear effects. Furthermore, exclusive-states are important input to the process of constructing new interaction theories. Most modern interaction theories cover only a limited portion of the phase space - perhaps they only predict the differential cross section for the final state lepton variables, or they only cover a small energy range, or they only cover either charged or neutral-current interactions. Exclusive state measurements help to over-constrain these models and promote revisions and improvements in the models.

The efforts outlined above all require measurements with both neutrinos and antineutrinos. With the opposite-sign axial-vector coupling, different initial-state particles at the hard scattering vertex, and the different overall cross-section, measurements with neutrinos alone are not sufficient to provide full kinematic coverage for an interaction model. Additionally, because antineutrinos sample different flavors of quarks, they provide a unique tool for measuring parton distribution functions.

MINERνA is uniquely capable of contributing to these measurements. By examining a range of nuclei in the same detector and the same beam, MINERνA can minimize systematic uncertainties by making measurements of ratios between nuclei to study A-dependent effects. It can also compare neutrino and antineutrino scattering to isolate different aspects of the primary interaction.

Comparisons between neutrino and antineutrino interactions are particularly important for model building. The final state interaction physics is nominally identical for neutrino and antineutrino interactions. So, comparisons between the two enable the untangling of nuclear effects due to the initial state and those that are in play in final state interactions.

2.2 Inclusive Measurements

Deep-inelastic scattering experiments utilizing charged lepton beams have firmly established that inelastic structure functions in nuclei differ significantly from those of free nucleons [2]. However, in spite of a program of intense theoretical [3, 4] and experimental work, there exists no universally accepted model that can describe these differences across all kinematic regimes. In order to shed new light on this situation, MINERνA has embarked on a program to measure cross section ratios between several different nuclei, ranging from lead and iron to scintillator (CH) and graphite. The first results from the Low Energy data, are already of sufficient precision to show significant A-dependent disagreements with predictions based on models informed by charged lepton measurements. A higher statistics exposure of both neutrino and anitneutrino data on the nuclear targets will enable an expansion of the kinematic range accessible.

The Medium Energy nuclear cross-section ratios as a function of the fractional momentum of the struck quark, x_{bj}, will not only be at higher precision than those taken in the Low Energy beam but will also have a different composition of quasielastic, resonance, and deep-inelastic (DIS) channels compared to the Low Energy beam sample. Observing how these new ratios differ from the Low Energy ratios in identical kinematic regions will by itself be helpful for understanding the physics behind those ratios.

The higher statistics and expanded kinematic range of the Medium Energy inclusive data will also enable the isolation of a statistically significant sample of DIS events. This will allow a measurement of neutrino-nucleus cross section ratios for carbon, iron and lead to scintillator (CH) in both the transition region (1.4 GeV $< W <$ 2.0 GeV) and in the DIS region with $W >$ 2.0 GeV, where W is the hadronic invariant mass. The x_{Bj}-dependent ratios of these DIS nuclear cross sections and nuclear structure functions will allow the examination of shadowing ($x_{Bj} \simeq 0.1$), anti-shadowing ($0.1 < x_{Bj} < 0.25$) and the EMC effect ($0.25 < x_{Bj} < 0.65$) in neutrino-nucleus scattering.

An earlier analysis of neutrino-Fe scattering from the NuTeV experiment [5], compared with a cross section model for neutrino-deuterium scattering, suggested that the nuclear ratios in these regions were quite different from the ones measured with charged-lepton-Fe scattering [6]. However, until MINERνA there has been no data available for direct comparisons between neutrino interactions measured on different nuclei. These ratios are some

of the most robust predictions of models and can clearly have the largest impact.

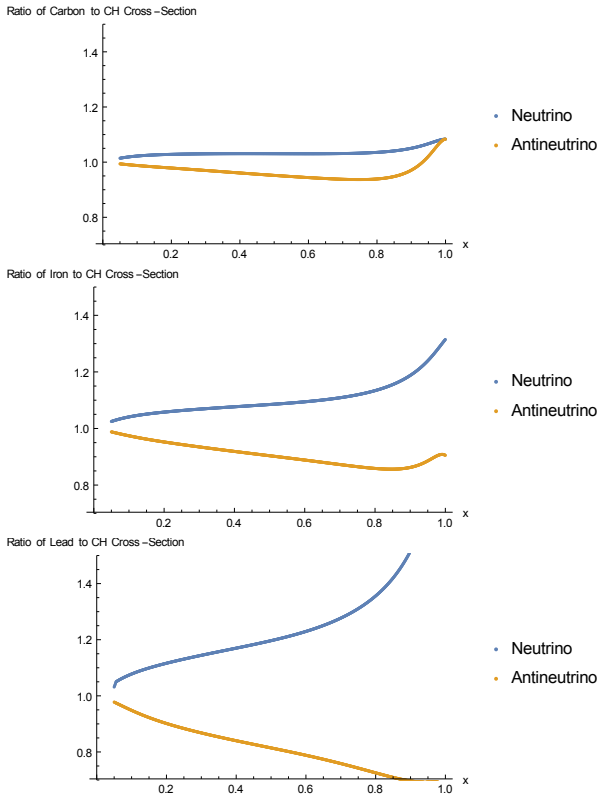

Figure 2: Cross Section Ratios in neutrino and antineutrino DIS for carbon (top), iron (middle), and lead (bottom) compared to scintillator, as predicted by a new model by Cloet [8, 9].

The work of Brodsky *et al.*[7] and the more recent work of Cloët *et al* [8] have emphasized the importance of quark flavor dependence of the nuclear effects described above. That neutrino and antineutrino scattering are sensitive to different combinations of quark flavors when compared to charged lepton scattering suggests that a difference in the measurements of these effects in neutrino and antineutrino scattering would shed new light on these effects.

Figure 2 shows the cross section ratios of Lead, Iron, and Carbon to scintillator (CH) as a function fo x_{Bj}, as predicted by Cloet [9]. The effects are

not only expected to be larger than what has been seen in charged lepton scattering, but are also expected to be very different in neutrino and antineutrino ratios. As will be demonstrated later in this document, MINERνA is well along the way towards achieving the required statistics in neutrino mode, and with 12×10^{20} Protons on target would also be able to measure the neutrino antineutrino differences.

3 Scientific Program

3.1 Low Energy Beam Physics Program

Most neutrino oscillation experiments rely on the final-state lepton kinematics to reconstruct both the neutrino energy and the momentum transfer to the nucleus (Q^2). MINERνA's first two publications were of the differential cross section for quasielastic scattering as a function of the muon-based Q^2 for neutrino [10] and antineutrino [11] modes, and a measure of the vertex energy distribution around both of those interactions [10]. MINERνA found that the most basic description of this process used by oscillation experiments does not reproduce either the Q^2 distribution the vertex energy distribution for neutrino quasielastic interactions. These data provide evidence for additional affects on the initial-state protons and neutrons in the nucleus that are not well-modeled.

MINERvA also isolated a sample of quasielastic-like events in the Low Energy beam with a tagged muon and zero pions where Q^2 was reconstructed only by final state proton kinematics. This measurement provides a new probe of the final state interactions. Comparisons with models show that the model that best matches the proton kinematics is not the same as the one that best predicts the muon kinematics [12]. The statistics in the Medium Energy beam will enable this analysis to be extended to the nuclear target region with several thousand events each on lead and iron, as described below.

Charged-current pion production is also an important process for oscillation experiments. For T2K analyses to date it represents a background that compromises the energy resolution of quasielastic candidates. For NOvA and future T2K analyses, as well as analyses in future experiments with fully active detectors, it is an important signal process whose rate and visible energy distribution must be understood. Although there are measurements of this process on deuterium, the predicted size of nuclear effects on this process

has not been confirmed by MiniBooNE's measurements on its hydrocarbon target. MINERνA measured this process on its hydrocarbon target in the Low Energy data. In this analysis, events with low hadron invariant mass squared (W) are chosen to enhance single pion production mostly from the $\Delta(1232)$, similar to the region measured by MiniBooNE. A comparison of the data to models shows the importance of including pion intranuclear rescattering. The cross section as a function of pion kinetic energy has a similar shape as MiniBooNE at lower neutrino energy, heightening the disagreement with theory seen previously [13].

Coherent pion production occurs when a neutrino interacts coherently with the entire nucleus and produces a forward charged or neutral pion. The neutral current version of this reaction is a rare but poorly known background for oscillation experiments, and the charged current version has been difficult to isolate in recent low energy neutrino experiments. K2K and SciBooNE did not observe coherent π^+ production at the level predicted by models in generators used by oscillation experiments. Upon selecting events with low momentum transfer to the nucleus, which is a model-independent signature of coherent interactions, MINERνA observes 1628 (770) coherent candidates in its neutrino (antineutrino) Low Energy data. It is found that the predicted coherent pion kinematics from neutrino event generators currently in use do not agree with the measured distributions, particularly for pions at large angles with respect to the neutrino beam [14]. Again the statistics expected in the Medium Energy beam will result in several thousand events of this kind on each of the lead and iron targets, thereby enabling an unprecedented study of the A-dependence of this process.

MINERνA's first measurement of nuclear effects comes from comparing inclusive neutrino charged current interactions on different solid targets. Figure 3 shows the cross-section ratios between iron and scintillator (left) and lead and scintillator (right) as measured by MINERνA in 3×10^{20} POT in the low energy beam [15]. The data show that as a function of the reconstructed variable $x_{Bjorken}$, which in the quark parton model corresponds to the fractional momentum of the struck quark, the nuclear effects measured differ significantly from expectations. The two kinematic regions where the data is not in agreement with the prediction correspond to different channels. The high $x_{Bjorken}$ behavior indicates nuclear effects near the quasielastic peak, while the low $x_{Bjorken}$ behavior indicates effects that may be present in pion production or deep inelastic scattering.

This measurement was limited by the statistics of the Low Energy run.

The current Medium Energy run will provide a 10-fold increase of events in neutrino running. With 6 (12) $\times 10^{20}$ POT in neutrino (antineutrino) mode, MINERνA will measure the cross section ratios as a function of $x_{Bjorken}$ with about 10^4 events in each of the bins shown in figure 3, in both neutrino and antineutrino modes.

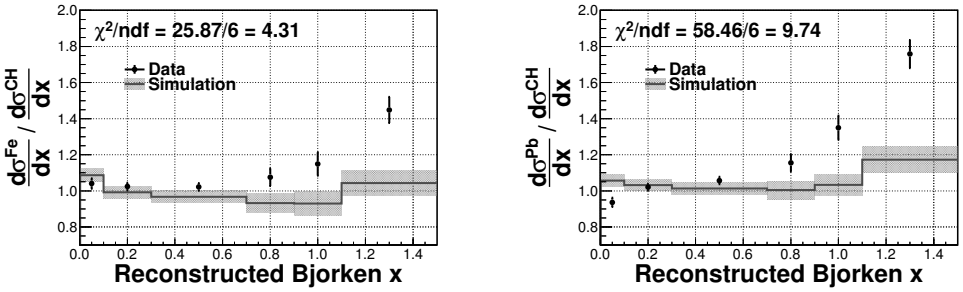

Figure 3: Cross-section ratios between iron and hydrocarbon (left) and lead and hydrocarbon (right) as a function of the fractional momentum of the struck quark in the parton model ($x_{Bjorken}$).

There are several important measurements that will come out of the Low Energy data set, covering precisely the peak neutrino energy region expected to be used by the future Long Baseline program. The antineutrino analog of the charged pion result described above, where a neutral pion is created in a charged-current interaction, will be released in January 2015. In addition, in the spring MINERνA plans to release its measurement of electron-neutrino CCQE interactions, which will be a first measurement of this extremely important cross section for electron neutrino appearance experiments. Finally, more detailed measurements of the quasielastic process in the scintillator as a function of muon kinematics, in both neutrino and antineutrino modes, is also in preparation for release in 2015.

3.2 Verifying the Medium Energy Data

3.2.1 Inclusive Charged Current Events

A high-statistics measure of the performance of the beamline and detector comes from looking at events that originate within the tracking volume of

MINERνA and project a muon that is tracked in the MINOS near detector. Fig. 4 shows the relative increase of events per proton on target in the Medium Energy beam compared to the Low Energy beam, as a function of muon energy. Clearly the flux increase shown in figure 1 is also accompanied by a total cross section increase as well, which means that for this inclusive sample the event rate per POT is a factor of 3.4 higher in the Medium Energy beam than that in the Low Energy beam.

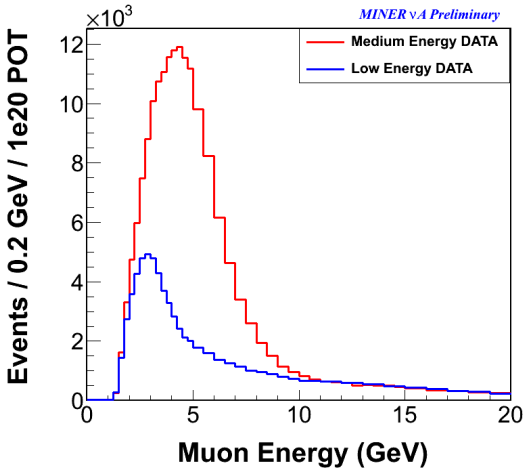

Figure 4: Muon momentum distribution for neutrino interactions in MINERνA per POT for the low energy and medium energy beams, showing the clear increase in measured event rates per POT.

The muon and the muon-equivalent non-track energies for the medium energy events are shown in Fig. 5, along with the prediction, normalized to the data. The time dependence of these quantities is also shown, indicating stability at better than a per cent over the first three months of the Medium Energy run.

3.2.2 Charged Pion Production in the Medium Energy beam

Because of the 3 ns timing resolution of the MINERνA electronics, the significant increase in events per 10 microsecond spill does not compromise MINERνA's ability to isolate exclusive channels in the Medium Energy data.

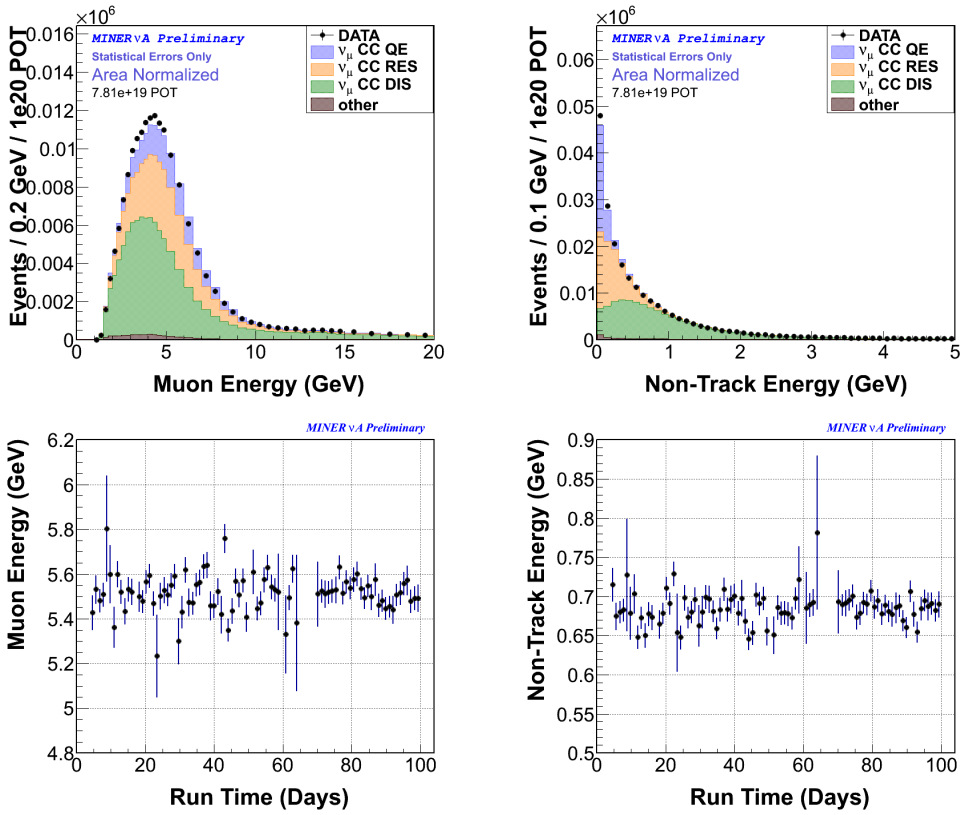

Figure 5: Top left (right): Muon (recoil) energy in the Medium Energy data and the prediction normalized to the data. Bottom Left (bottom right): Muon (recoil) energy as a function of time for the 3 months of the first part of the Medium Energy run.

Figure 6(left) shows the current status of the charged current pion production analysis in the Medium Energy beam. Events in this sample contain a muon that is tracked into MINOS, together with an additional track originating from the vertex that is identified as a charged pion. Additionally, the Michel electron that comes from the pion decay must also be found at a later time during the spill, and the invariant mass of the final state hadronic system must be below 1.4 GeV to correspond to single pion production. The simulation shown in the Figure includes the accidental activity present in the Medium Energy run. The data are for 0.8×10^{20} protons on target; the simulation is normalized to the data. Figure 6(right) shows the vertex distribution along the beamline axis for the multi-pion production analysis to increase statistics. The change in acceptance as a function of vertex position for this process is well-modeled in the simulation.

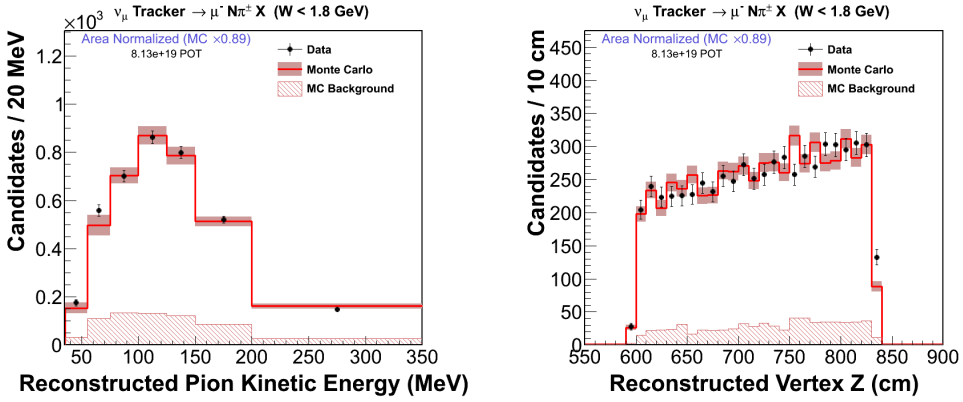

Figure 6: Left (Right): Pion kinetic energy (Z vertex) distribution for Medium Energy data and simulation, where the simulation has been normalized to the data event rate.

Based on the change in acceptance shown in Fig. 6, there would be several hundred events estimated to be collected in the nuclear target region, enabling the cross section ratios for this exclusive process between Iron or Lead to scintillator to be measured to an accuracy of 5%.

3.2.3 Beamline and Detector Performance over Time

To verify both the detector and beamline performance several types of event rates per POT have been measured over the run. The rate of muons per

POT in the MINERνA detector that originate from upstream neutrino interactions, and the rate of muons matched to the MINOS near detector are two high statistics indicators that the two detectors' tracking and relative timing capabilities are stable over time. The rates also indicate whether the NuMI beamline is producing neutrinos at a constant rate. However, there is still a few percent intensity dependence to the number of reconstructed muons, so the protons delivered per spill must also be considered. Figure 7 shows these event rates and protons per pulse throughout most of the Medium Energy run. The small 1-day deviations reflect problems with the proton accounting system. The few percent deviation around March 2014 is evidence of the intensity dependent effects that must be simulated in the Monte Carlo.

3.2.4 Scintillator Aging

A sensitive measure of the health of the MINERνA detector over time is the average or peak number of photoelectrons collected when a muon crosses a scintillator plane. Over time, scintillator ages and produces less light for the same energy deposited. The light yield histories for both the MINOS and MINERvA detectors are shown in figure 8. Both detectors exhibit an exponential decay in the light yield, as expected. The large gap starting at 2.2 years for the MINERνA plot represents the year-long shutdown to switch between the Low and Medium Energy configurations. There was a ten degree shift in the temperature in the hall, which changed the rate of light loss as a function of time. Before the cooling upgrade the light levels for MINERvA (MINOS) were dropping at 7.4% (3.5%) per year. After the cooling upgrade through the current run the MINERνA (MINOS) scintillator light yield is dropping at a rate of 4% (2.1%) per year. At the beginning of the Low Energy run the MINOS near detector scintillator was producing on average 6.4 photo-electrons per normally incident minimum ionizing particle [16].

Part of the MINERνA detector prototyping involved doing a "vertical slice test" using three stacked planes each comprised of 7 of MINERνA's scintillator extrusions between two paddles comprising a cosmic ray trigger system. A systematic study was performed to measure the position resolution of the scintillator planes as a function of light loss (provided by neutral density filters). Based on those results and the current rate of light yield loss, MINERvA's position resolution in another 13 years (March 2023) will have degraded by about 30% compared to its initial light levels citevst.

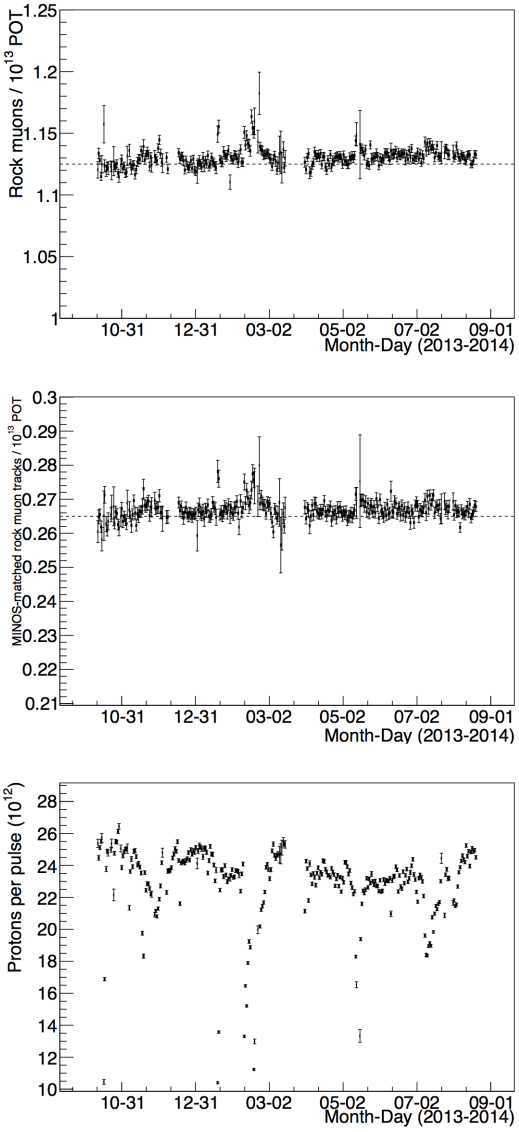

Figure 7: Rock muons per POT in MINERνA (top) and in MINERνA that are matched to tracks in the MINOS near detector (middle), for a given protons per pulse (bottom) as a function of time during the Medium Energy run. The rates of reconstructed tracks per POT is observed to be constant in time for both detectors (top and middle) for all periods of running with a "healthy" ($> 20 \times 10^{20}$ POT) beam intensity (bottom plot).

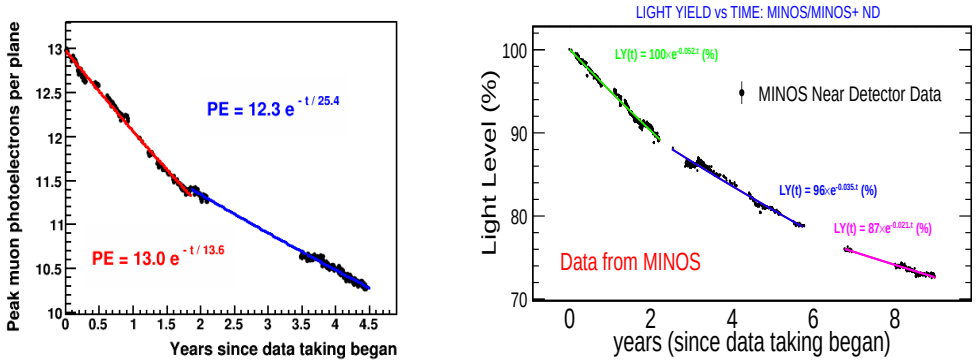

Figure 8: Left: MINERvA's average photoelectrons collected for a minimum-ionizing track at normal incidence to a scintillator plane, as a function of time as measured in years past the start of MINERA's Low Energy run (March 2010). Right: MINOS Near Detector light yield as a function of time, normalized to the beginning of the MINOS Low Energy run (May 2005).

3.3 MINERvA's Test Beam Program

An important component of MINERvA's Low Energy neutrino interaction program was a test beam program measure the response of a smaller version of the MINERνA detector to hadrons at the tertiary beam of the Fermilab Test Beam Facility. This beamline provided protons, pions, kaons of energies ranging from 400 MeV to 2 GeV, and electrons from 400-600'MeV . Upstream instrumentation was used for particle identification and precise momentum measurement of the incoming particles. The detector response was measured in two configurations to study the three different regions of the MINERνA detector: the all scintillator region used for tracking, as well as the electromagnetic and hadronic calorimetry sections. Measurements were made to verify the accuracy of the detector simulation of proton, pion, and electron calorimetry, as well a to perform a study of tracking efficiency for protons and measure Birks' law parameter of the MINERνA scintillator. The two plots in Fig. 9 show the detector's response to pions are modeled by the simulation to better than 5% and are used to constrain the absolute energy scale for low energy pions.

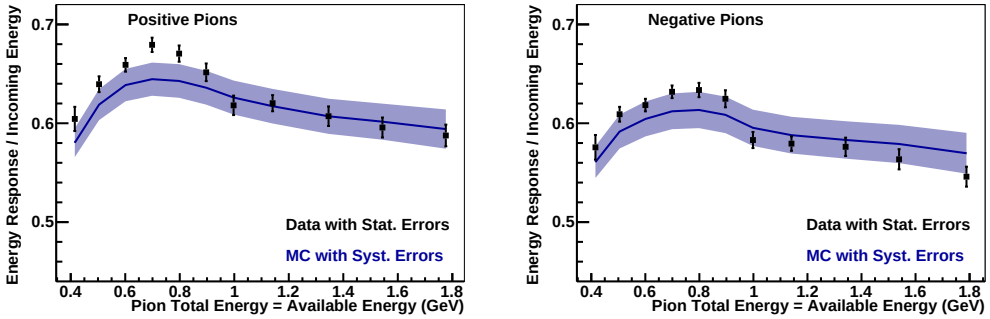

Figure 9: Calorimetric response for positive (left) and negative (right) pions. The errors on the data are statistical only, while the error band on the MC represents the systematic uncertainties on comparisons between data and simulation. A larger uncertainty of up to 4.2% (not shown) applies to the absolute response scale both data and simulation.

In the Medium Energy neutrino beam, however, there will be hadrons of higher energies not available in the tertiary beam. To address the overall hadronic energy scale for hadrons and for a better measurement of the detector response to electrons MINERνA is currently commissioning its test beam detector in the secondary hadron beam at the Fermilab Test Beam Facility. MINERνA will take data in the Winter of 2015 in several detector configurations to again map out the response of both the tracking and calorimeter sections of the detector but using hadron and electron energies up to 10 GeV.

4 Physics Reach in the Medium Energy Beam

Because of the high statistics of many exclusive samples in the Medium Energy data set, an accurate flux prediction is even more important than it is for the Low Energy exposure. This section first describes the techniques that MINERvA plans to use to reduce the flux uncertainty below what it has been for our first Low Energy publications, and then describes the expectations for the physics reach of some of the key Medium Energy analyses. Getting the lowest flux uncertainty through neutrino electron scattering will require full statistics in neutrino mode, as will getting to the most precise measurements of nuclear effects in neutrino scattering.

4.1 Flux Uncertainties

The integrated energy-weighted neutrino flux can be known in the Medium Energy beam to about 5% or better in neutrino mode. This is because of the high statistics expected in neutrino-electron scattering events, whose cross section is known precisely. A preliminary analysis on 0.8E20 POT with the same selection critieria used in the low energy beam is shown in Fig. 10. The critical observable for isolating these events, the electron energy times the square of the angle with respect to the beam is plotted on the left. Already with a preliminary calibration with known offsets and the preliminary flux estimate, the resolution on this variable is reasonably well-modeled. The right plot shows the electron energy distribution for events passing an $E_e\theta^2$ cut.

These plots show that even in the high instantaneous event rate in the Medium Energy beam, the detector is capable of isolating these rare events. For an exposure in neutrino mode of 10×10^{20} POT the experiment would collect roughly 1100 events.

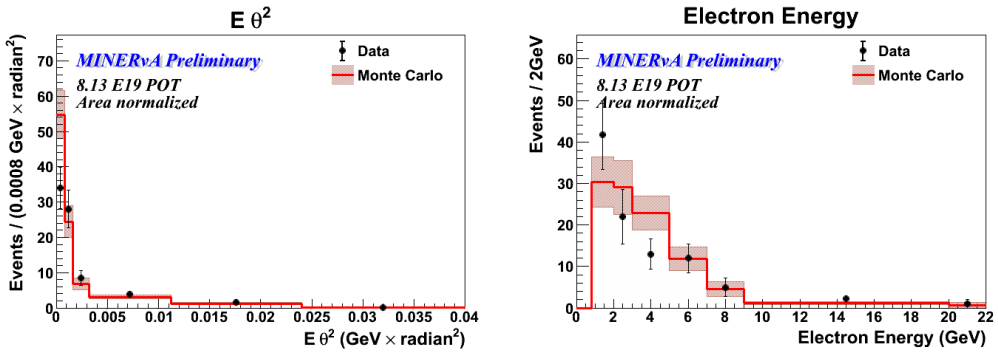

Figure 10: Left: Electron energy times the square of the angle with respect to the beam ($E_e\theta^2$) for a portion of the Medium Energy data, for events with an electron candidate and very little other activity in the detector. Right: Electron energy distribution for events passing a cut on $E_e\theta^2$ to remove backgrounds.

The MIPP measurements of pion production on a NuMI replica target[18] will also be used to further constrain the flux prediction. These measurements, which are currently being incorporated into MINERνA's Low Energy

flux prediction, have a 3-4% statistical uncertainty in the relevant pion production kinematic region for the NuMI Medium Energy beam, and a 4-5% systematic uncertainty. The MIPP experiment's measurements cover the portion of pion phase space relevant to both the Low and Medium Energy beams; so, the infrastructure to incorporate those data now will be used to constrain both flux predictions.

Taken together, these two constraints will improve the Medium Energy flux uncertainties well below those currently in place for the Low Energy beam.

4.2 Charged Current Quasi-elastic scattering

MINERνA has a unique opportunity to measure the nuclear effects that govern exclusive interactions. The Medium Energy exposure offers a large increase in statistical precision over the Low Energy exposure as well as the chance to measure the energy dependence of nuclear effects. Figure 11 shows the event samples for the Low Energy beam, and predictions for the Medium Energy beam. In the Low Energy plots of Fig. 11 the simulation has been normalized to the data. The backgrounds from inelastic processes are not significantly worse in the Medium Energy beam, as shown in the plots. The backgrounds from scintillator events in the iron and lead samples are comparable in the Low and Medium Energy data and estimated at about 20% of the sample.

For an exposure of 6×10^{20} POT, MINERνA expects to collect about 6600 2-track quasielastic candidates on the graphite target, as well as over 47,000 and 44,000) 2-track quasielastic candidates on the iron and lead targets respectively. Given the 17% scintillator contamination, this would mean a statistical uncertainty at the 3 percent level. Although the non-quasielastic background is still substantial, with these statistics a sideband approach to study that background can be used, similar to what was done in the scintillator analysis in the low energy beam [12].

4.3 Charged Current Coherent Pion Production

Extending the charged-current coherent pion analysis to the Medium Energy exposure would greatly extend the statistical precision of this rare process. Figure 12 shows that the same variable that was used in the Low Energy data to isolate the signal can be well-reconstructed in the Medium Energy

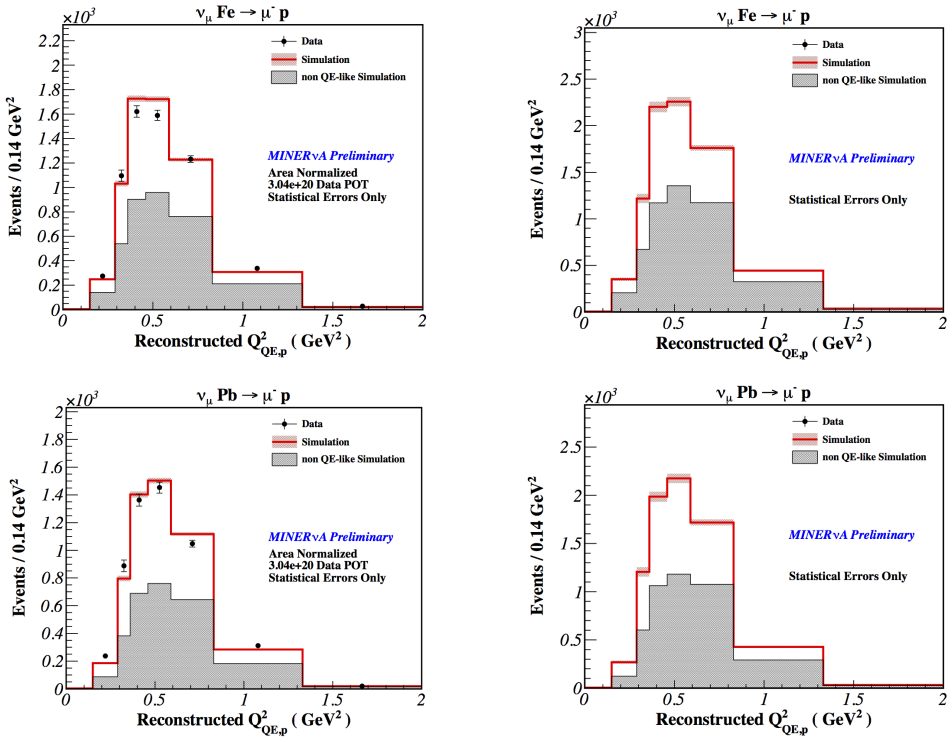

Figure 11: Momentum transfer squared, as measured by the outgoing proton kinetic energy, for the Low Energy data and simulation (left) and projected for 1×10^{20} POT in the medium energy simulation (right), for events originating in iron (top) and lead (bottom) nuclei. Backgrounds from inelastic processes are shown in the shaded regions.

data which naturally has more inelastic events in the sample and potentially more background (and higher energy events, which means the tracks are even more boosted in the forward direction). This analysis predicts that the non-coherent background in the Medium Energy data will be comparable to that in the Low Energy data, and that the event rate per proton on target will be 3.5 (3.4) times as large in neutrino (antineutrino) mode. This means that with 10×10^{20} (12×10^{20}) protons on target in neutrino (antineutrino) mode, the experiment expects to increase the coherent statistics by a factor of 11 (24), and measure the cross section at higher energies.

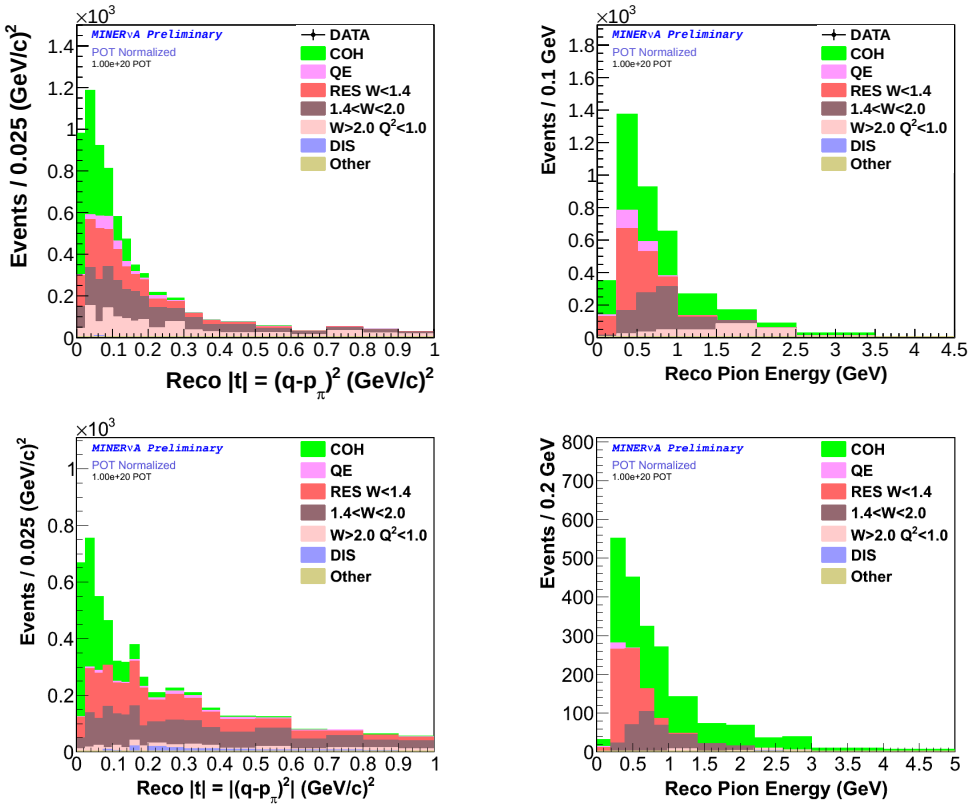

Figure 12: The momentum transfer to the nucleus (left), and pion energy distribution (right), predicted for the Medium Energy neutrino (top) and antineutrino (bottom) data, for 1×10^{20} POT.

By scaling the relative masses of the most downstream nuclear target

materials to the scintillator mass (2.7% and 2.2% for iron and lead respectively), the number of coherent events collected on iron and lead is estimated to be above 200 in each mode, as shown in Table 1. Additional statistics on lead would be available using an additional nuclear target. Actually, it is not known how the cross scales as A. It could scale as $A^{1/3}$ or $A^{2/3}$, and the MINERνA data should be able to discriminate between the two.

Mode	Scintillator	Iron Target 5	Lead Target 5	Lead Target 4
Neutrino	11,000	310	240	420
Antineutrino	21,000	570	450	790

Table 1: Statistics in the Medium Energy beam for Coherent pion events in neutrino and antineutrino mode, for the scintillator and the most downstream nuclear targets. These projections assume 6×10^{20} (12×10^{20}) POT in neutrino (antineutrino) mode.

4.4 EMC Effect in Neutrino Scattering

Finally, the Medium Energy data will allow an unprecedented study of nuclear effects in deep inelastic neutrino scattering. Figure 13 shows the true x_{Bj} distributions for an exposure of 1×10^{20} POT. These events have passed all anaysis cuts to isolate a charged current signal on the iron nuclear target in both the neutrino and antineutrino beam, for an inclusive sample. The ratio of events in antineutrino compared to neutrino is about a factor of two, as expected, and the inclusive event sample is comprised of many different kinds of interactions.

The EMC effect itself has been measured in Deep Inelastic Scattering processes in electron scattering experiments, and in order to probe the nuclear effects on the quarks themselves a cut to isolate the DIS events must be made. Figure 14 shows the event samples in iron after a cut requiring the reconstructed momentum transfer squared to be above 1 GeV and the invariant hadron mass is required to be above 2 GeV. Note that the events per POT for the antineutrino sample has now dropped to roughly a fifth that of the neutrino statistics. The ratios of events on lead are again comparable to those on iron, while those on carbon are again a factor of three lower and those on scintillator are a factor of 10 higher.

The most stringent tests of the models will be to compare the cross section ratios between different materials, for both neutrino and antineutrino

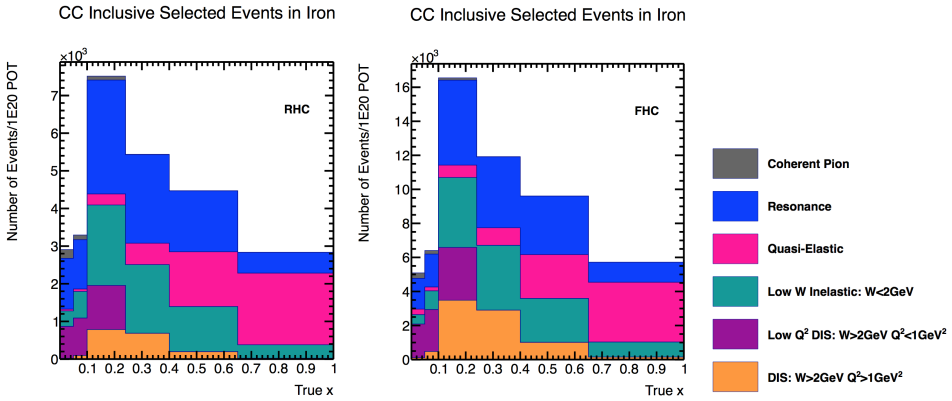

Figure 13: x_{Bj} distributions per 1×10^{20} POT for accepted events on iron in the medium energy neutrino and antineutrino beams.

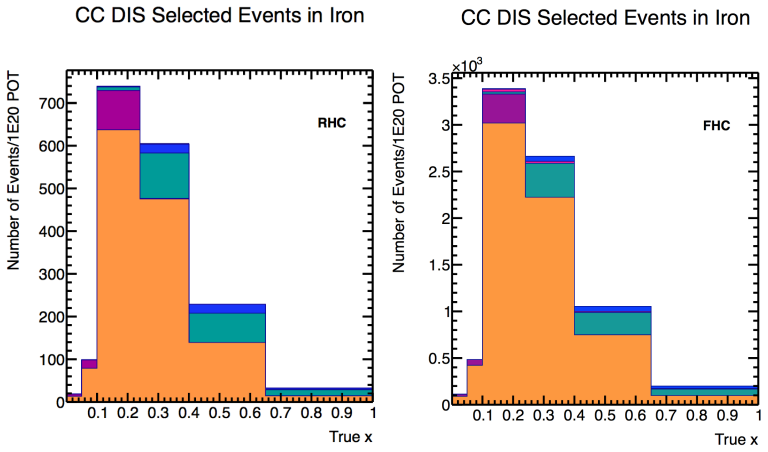

Figure 14: x_{Bj} distributions for accepted events on lead for neutrino (left) and antineutrino (right) running, after a cut is made to isolate DIS events, per 1×10^{20} POT in the medium energy neutrino (antineutrino) beam.

interactions. For the antineutrino ratios, the DIS cross section above x of 0.4 will be most sensitive to u quark distributions, while the for neutrino rates will be most sensitive to the d quark distributions. At lower x_{Bj} MINERνA will have a handle on what in electron scattering is called the shadowing region. By measuring the cross setion ratios for three different nuclei and over range of different x_{Bj} values MINERνA will be able to get a first glimpse of the quark dependence of the EMC effect.

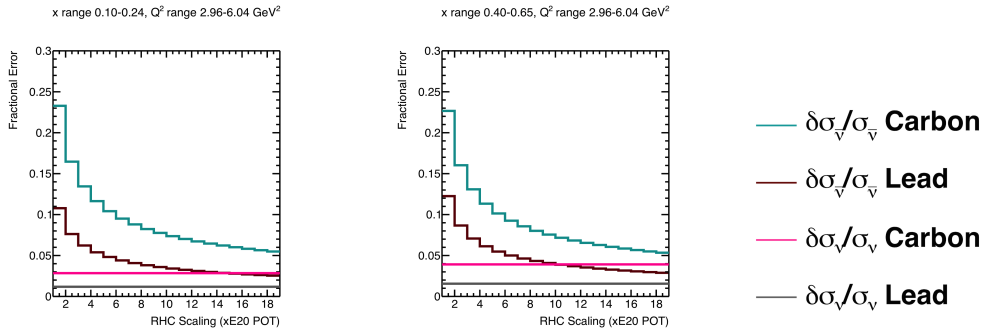

Figure 15: Fractional uncertainties on antineutrino cross sections on Carbon and Lead for Q^2 between 3 and 6 GeV^2 for low (left) and high (right) X_{Bj} bins, as a function of antineutrino integrated POT, compared to the neutrino cross section uncertainties for an exposure of 10×10^{20} POT.

The fractional uncertainties on the cross section ratio on lead and carbon to scintillator as a function of antineutrino POT are shown in comparison to the statistical uncertainty on the neutrino cross section for that same nucleus in Fig. 15. Even for an exposure of 12×10^{20} POT the cross section uncertainties will not be the same, but they will be close to the 5% level.

MINERνA's best sensitivity to the EMC effect comes from integrating over all Q^2 values in each X_{Bj} bin, and is shown in Fig. 16. The uncertainty on the cross section ratio between scintillator and iron is similar to that of lead, and both cross section ratios to scintillator can be measured to roughly 5% in the three intermediate X_{Bj} bins. The fractional uncertainty for the iron to scintillator ratio, not shown, is expected to be within 5% of that of lead due to the similar masses of the nuclear targets. The systematic uncertainties on these ratios in the Low Energy analysis were at the 5% level or less, and were dominated by background subtraction. But only with

12×10^{20} POT in antineutrino mode can the statistics in carbon become as low as the systematic uncertainties. By comparing the uncertainties in Fig. 16 to the predictions in Fig. 2 it is clear that MINERνA is poised to confirm or refute the prediction of partity-violating nuclear effects.

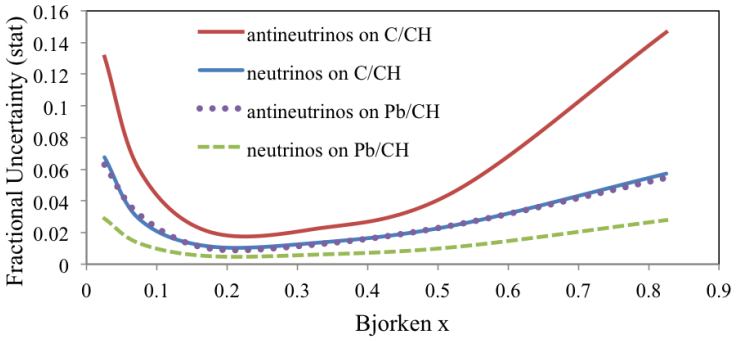

Figure 16: Fractional uncertainties on neutrino and antineutrino cross section ratios to scintillator for Carbon and Lead as a function of X_{Bj} bin, for an exposure of (12×10^{20} POT) in neutrinos (antineutrinos).

4.5 Conclusions

MINERνA, with its low energy neutrino and antineutrino exposures, is advancing our knowledge of neutrino-nucleus interactions with its recent and on-going measurements of quasielastic scattering, charged current pion production, coherent pion production, and A-dependence of inclusive charged-current scattering. As documented in this Report, the MINERνA Collaboration has clear evidence that the medium energy ν_μ scattering data currently being recorded is of excellent quality. Extended running with ν_μ and $\bar{\nu}_\mu$ in the NuMI medium energy mode presents abundant opportunities to compliment and to significantly extend its investigations of fundamental neutrino-induced processes.

References

[1] L. Aliaga *et al.* (MINERvA Collaboration), Nucl. Instrum. Meth. **A743** 130-159, (2014).

[2] J. J. Aubert *et al.* [European Muon Collaboration], Phys. Lett. B **123**, 275 (1983).

[3] B. Z. Kopeliovich, Nucl. Phys. Proc. Suppl. **139**, 219 (2005) [hep-ph/0409079].

[4] J. W. Qiu and I. Vitev, Phys. Lett. B **587**, 52 (2004) [hep-ph/0401062].

[5] M. Tzanov *et al.* (NuTeV Collaboration) Phys. Rev. **D74**, 012008 (2006).

[6] K. Kovarik, I. Schienbein, F. I. Olness, *et al.*, Phys. Rev. Lett. **106** 122301 (2011)

[7] S. J. Brodsky, I. Schmidt and J. J. Yang, Phys. Rev. D **70**, 116003 (2004) [hep-ph/0409279].

[8] I. C. Cloet, W. Bentz and A. W. Thomas, Phys. Rev. Lett. **109**, 182301 (2012) [arXiv:1202.6401 [nucl-th]].

[9] I. C. Cloet, private communication

[10] G. A. Fiorentini, D. W. Schmitz, P. A. Rodrigues *et al.* (MINERvA Collaboration), Phys. Rev. Lett. **111**, 022502 (2013).

[11] L. Fields, J. Chvojka *et al.* (MINERvA Collaboration), Phys. Rev. Lett. **111**, 022501 (2013)

[12] T. Walton, M. Betancourt *et al.* `hep-ex 1409.4497` submitted for publication

[13] B. Eberly *et al.* `hep-ex 1406.6415`, submitted for publication

[14] A. Higuera, A. Mislivec *et al.*, hep-ex 1409.3835 to appear in Phys. Rev. Lett.

[15] B.Tice *et al.* Phys. Rev. Lett. **112**, 231801 (2014).

[16] MINOS position paper on Calibration, MINOS docdb 1289 (2006).

[17] J. Chvojka, MINERvA-docdb 1592, (2007).

[18] J. M. Paley, M. D. Messier, R. Raja *et al.* Phys. Rev. **D90** 032001 (2014)